Journal of Basic Physical Research ISSN: 2141-8403 Prints, 2141-8411 Online
Vol.11, No.1 pp. 45- 62, March., 2023. Available online at www.jbasicphyres-unizik.org

STRUCTURAL FRAMEWORK AND HYDROCARBON POTENTIAL OF THE AGBOMA FIELD, ONSHORE NIGER DELTA BASIN, NIGERIA.

Aitonje, E.[1*], Ahaneku, C. V.[1,2], and Ajaegwu, N. E.[1]
[1] *Department of Geological Sciences, Nnamdi Azikiwe University, Awka, PMB 5025, Anambra State, Nigeria.*
[2] *Marine Geology and Seafloor Surveying, Department of Geosciences, University of Malta, Msida, MSD 2080, Malta.*

Abstract
This study presents an integration of seismic attributes and petrophysical analysis for the re-evaluation of the hydrocarbon potential of the Agboma Field, Onshore Niger Delta Basin, using 3-D seismic reflection data and a suite of geophysical well-logs. The Agboma Field has experienced a steady decline in hydrocarbon production at an average of 42% over the last five years. Understanding the trapping mechanisms, reservoirs' vertical and lateral extent, quality and connectivity within the Agboma Field forms the basis for this research. The methods employed include lithofacies and petrophysical analysis of the well-logs, seismic-to-well tie, volume and surface attribute analysis, fault and horizon mapping, layer cake velocity model, time-depth conversion and prospect evaluation. The lithofacies analysis and correlation of the delineated facies show that the reservoirs vary in thickness and are laterally continuous across the field. Four hydrocarbon-bearing reservoirs named AMR-1, AMR-2, AMR-3, and AMR-4; and one prospect reservoir named AM-Prospect reservoir which is the major contribution of this study were identified and correlated. Petrophysical analysis indicates that the sandstones generally have excellent reservoir quality with an average effective porosity of 26% permeability of 715 mD and hydrocarbon saturation of 74%. The AM-Prospect reservoir has a net-to-gross of 100% and is commercially viable for increased oil production within the Agboma Field with Stuck Tank Oil Initial In Place (STOIIP) of 341 MMSTB and 362 MMSTB for AM Prospect 1a and 1b respectively. The structural interpretation shows that the Agboma Field is characterized by four down-to-basin normal faults that compartmentalized the field into four blocks labelled blocks A to D. The reservoir structural map document fault-dependent and rollover anticlinal structural closures that show high RMS amplitudes conforming to structures in the undrilled blocks B and C and interpreted as AM Prospect 1a and 1b. The results of this studydemonstrate the importance of integrating petrophysics, seismic attributes and structural framework analysis in evaluating oldhydrocarbon-producingg fields for increased hydrocarbon production.
Keywords: *Structural Framework, Petrophysics, Niger Delta Basin, Seismic Attributes, Reservoir, Hydrocarbon Potential.*

Introduction

The Niger Delta Basin has been a critical area for hydrocarbon exploration following the first exploration activities by Shell-BP in 1956. Since then, the basin has received overwhelmingscientific research and exploration activities. It ranks among the world's most prolific petroleum-producing Tertiary deltas, which accounts for about 5% of the world's oil and gas reserves (Aniefiok *et al*., 2013). Investigations have shown that within the last ten years, Nigeria's energy reserves have declined due to the limited number of new discoveries within the basin. Only 2% of Niger Delta wells have reached deeper than 15,000 feet total depth; and 70% of the wells in the basin have not gone deeper than 9000 feet True Vertical Depth (TVD) (Omatsola, 2013). This simply means that the Niger Delta basin still holds frontier exploration locations where new fields can be discovered and existing fields can be re-evaluated using integrated techniques for hydrocarbon production optimization. Omatsola (2013) concluded that the reassessment of existing fields will greatly increase the hydrocarbon reserve base of Nigeria's energy sector. According to the field assessment report, the Agboma Field, Onshore Niger Delta basin has been experiencing a steady decline in hydrocarbon production at an average of 42% from seven producing wells that targeted different structural closures within the field.

Hydrocarbon-charged sediments detection and characterization is the primary concern of petroleum exploration and production companies. A petroleum reservoir represents a heterogeneous subsurface geological system with considerable intrinsic complexities. These complexities range from natural heterogeneity of reservoir facies, uncertainty and nonlinearity in reservoir parameters, and structural complexities within the reservoir area. As new fields have become hard to find and exploration & production costs increase with the decrease in the price of crude, stakeholders in the oil and gas industry have responded by revisiting marginal fields. The aim is to effectively and efficiently extract more information from available data and discover new prospects using integrated techniques. The philosophy of discovering new prospects involves the integration and calibration of seismic data with available well data. The use of seismic attributes derived from seismic data has received considerable attention for reservoirs characterization, especially in defining reservoir properties and offers reliable solutions to the perceived reservoir problems within old producing fields (Ahaneku et al., 2016; Nwaezapu et al., 2017; Obiadi et al., 2019). Seismic amplitude which represent primarily contrasts in elastic properties between individual layers contain information about lithology, posority, pore fluid type, and saturation – information that cannot be gained without integrating seismic attributes, well-logs and 3-D structural interpretation.

This study aims to re-evaluate and identify new hydrocarbon leads and prospects within the Agboma Field in the Coastal Swamp depobelt, onshore Niger Delta Basin, Nigeria by integrating petrophysical, seismic attribute and structural analysis. The objectives of the study were to (1) identify the hydrocarbon-bearing sand units, calculate and compare petrophysical properties such as permeability, porosity, net-reservoir thickness, net-to-gross, water saturation and hydrocarbon saturation for each reservoir sand unit in each of the wells used in this study. (2). Build a robust structural framework of the field and identify new hydrocarbon prospects using seismic attributes and structurapingping, and (3) Evaluate identified prospects based on exploration risks. This study contributes to the existing literature for optimizing hydrocarbon production within marginal fields in the Niher Delta Basin and across the globe.

Geology of the Study Area

The Niger Delta Basin is Paleocene in age and originated from the opening of South Atlantic as a result of the rifting and separation of South American and African tectonic plates. The Benin Flank marks the western limit of the basin. Cretaceous sediments of the Anambra and the Abakaliki Basins define the northern boundary while the Calabar Hingeline marks the eastern limits (Reijers *et al*., 1997). The three major stratigraphic units include the marine Akata Formation, the fluvial-deltaic Agbada Formation and the continental Benin Formation (Doust and Omatsola, 1990). After rifting, gravity tectonism became the primary deformational process. Shale mobility induced internal deformation occurred in response to two processes (Kulke, 1995). First, shale diapirs formed from loading of poorly compacted, overpressured, pro-delta and delta-slope clays (Akata Formation) by the higher density delta-front sands (Agbada Formation). Second, slope instability occurred due to a lack of lateral, basin-ward support for the undercompacted delta-slope clay (Akata Formation). For any given depobelt, gravity tectonics were completed before deposition of the Benin Formation and are expressed in complex structures, including shale diapirs, rollover anticlines, collapsed crest structures, back-to-back features, and steeply dipping, closely spaced flank faults (Figure 1) (Evamy *et al*., 1978; Xiao and Suppe, 1992). These faults mostly offset different parts of the Agbada Formation and flatten into detachment planes near the top of the Akata Formation. Deposition of the three formations occurred in each of the five off-lapping siliciclastic sedimentation cycles that comprise the Niger Delta. Evamy *et al*., (1978) recognized five mega-sedimentary zones; Northern Depobelt, Greater Ughelli Depobelt, Central Swamp Depobelt, Coastal Swamp Depobelt and the Offshore Depobelt. Each of the zones constitutes a separate province in terms of time-stratigraphy, deformation style, sedimentary facies, and generation and migration of hydrocarbon (Evamy *et al*., 1978).

These depobelts are defined by syn-sedimentary faulting that occurred in response to variable rates of subsidence and sediment supply (Doust and Omatsola, 1990). Each depobelt is a separate unit that corresponds to a break in regional dip of the delta and is bounded landward by growth faults and seaward by large counter-regional faults or the growth fault of the next seaward belt (Evamy et al., 1978; Doust and Omatsola, 1990). Doust and Omatsola (1990) describe three depobelt provinces based on structure. The northern delta province, which overlies relatively shallow basement, has the oldest growth faults that are generally rotational, evenly spaced, and increases their steepness seaward.

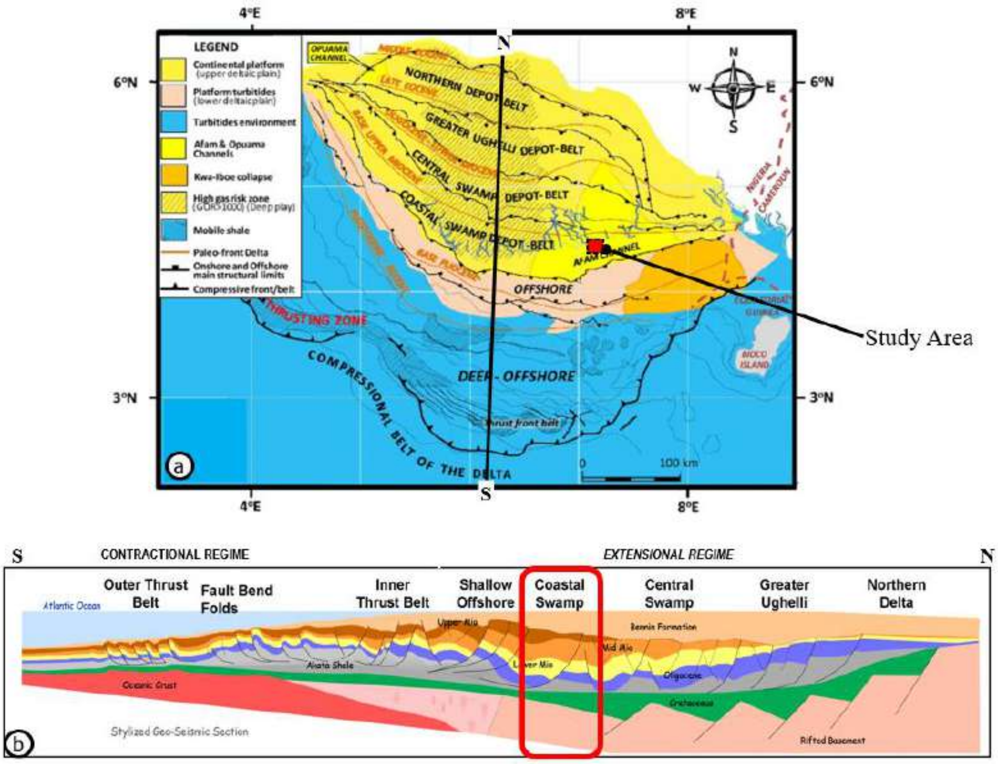

Figure 1: Schematic Niger Delta regional dip cross-section showing structural belts, depobelts and stratigraphy of the Niger Delta basin. Figures a and b modified from Nwozor *et al.,* (2013) *and* Ajakaiye and Bally, (2002) respectively.

The Tertiary Niger Delta is characterized by syn-sedimentary gravitational growth faults, developed as a result of rapid sand deposition and differential loading of coarser clastics over fine-grained under-compacted marine shales of the Akata Formation (Ajakaiye and Bally, 2002). Evamy *et al*. (1978) described the fault types commonly found in the Niger Delta Basin include normal growth faults, down-to-basin listric normal faults, synthetic and antithetic normal faults, rollover anticlines and diapirs. The growth faults are contemporaneous and more or less continuously active with deposition such that their throws increase with depth. The growth faults may be listric, typically cuspate normal faults, which flatten with depth into the thick clastic shaly sequence of the Akata Formation. Continuous growth of the faults after their inception, allows for greater sedimentation on the down-thrown blocks relative to the upthrown blocks. This syn-sedimentary tectonic activity in the Niger Delta Basin gave rise to structural deformations, producing series of fault blocks (Figure 1b). Intense folding of the sediments and thrust faulting are prominent processes in the offshore Niger Delta where translational and compressional structures are well developed due to rapid sediment influx and consequent gravity tectonics (Ajakaiye and Bally, 2002).

The study area is onshore within the southeastern Coastal Swamp depobelt, Niger Delta Basin, Nigeria. It lies between Longitudes 7° 10' 41.87" E and 7° 22' 29.11" E and Latitudes 4° 23' 52.38" N and 4° 36' 16.15" N (Figure 2). The study area lies within the Coastal Swamp Depobelt which is a shelfal and deltaic setting in the Middle to Late Miocene where sea-level changes had a great impact on the quality, development, and distribution of reservoir and seal facies and other petroleum systems elements in the basin (Short and Stauble, 1977; Doust and Omatsola, 1990; Ogbe 2020). The field was discovered in 1991 by Shell Petroleum Development Company (SPDC) Nigeria Limited after the completion of AM-1 well that targeted a structural prospect and with the acquisition and processing of Agboma 3-D seismic reflection data. Commercial hydrocarbon production from the field commenced in 1992 by drilling AM-2 production well.

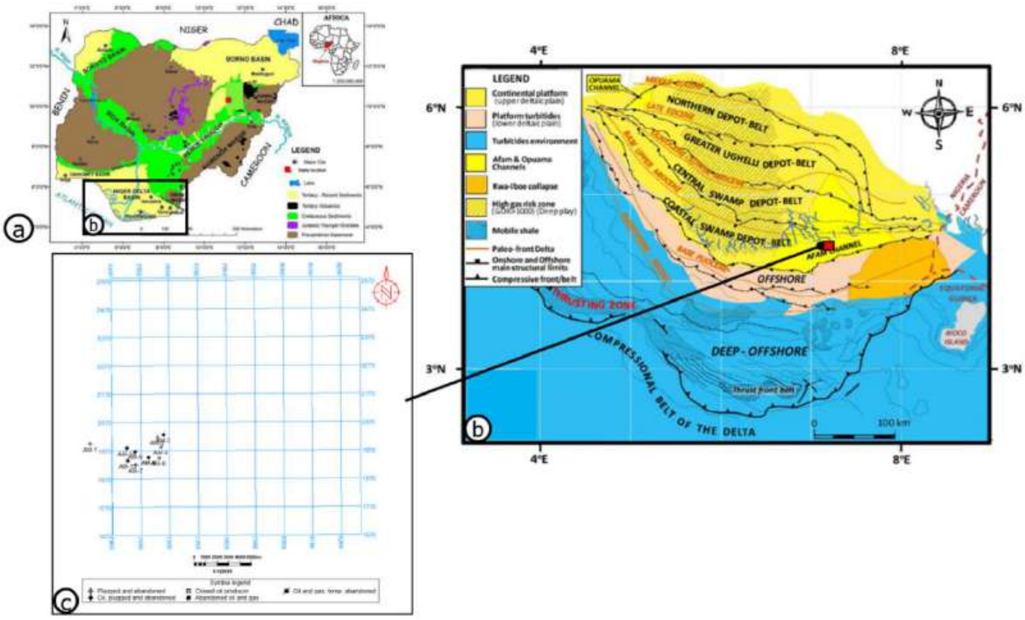

Figure 2: Location map of the study area. (a) Map of Nigeria and Africa (insert). (b) Map Niger Delta Basin showing depobelts and location of Agboma Field (modified from Nwozor et al. 2013). (c) The base map of Agboma Field shows the locations of the wells used in this study.

Materials and Methods

The data set for this study was made available by Shell Petroleum Development Company (SPDC), Port Harcourt, Nigeria. The data consists of a 3-D seismic reflection volume (Figure 3), nine wells with full log suites, checkshot data for four wells and biostratigraphic data for two of the wells provided (Table 1). The seismic data used for this study is a 149.34 km^2 post-stack, time migrated reflection seismic volume stored in SEG-Y format. The 3-D seismic displayed as zero phase, SEG normal polarity where a peak represents increasing acoustic impedance coloured blue (positive amplitude) and a trough represents decreasing acoustic impedance coloured red (negative amplitude). The seismic data has a dominant frequency of 23 Hz. The reflection quality of the data is good. The 3-D seismic volume was interpreted for stratigraphic and structural analysis as well as for hydrocarbon prospect evaluation. The borehole data were interpreted for the lithofacies analysis, reservoir evaluation, petrophysical analysis of the reservoir properties and generation of synthetic seismogram.

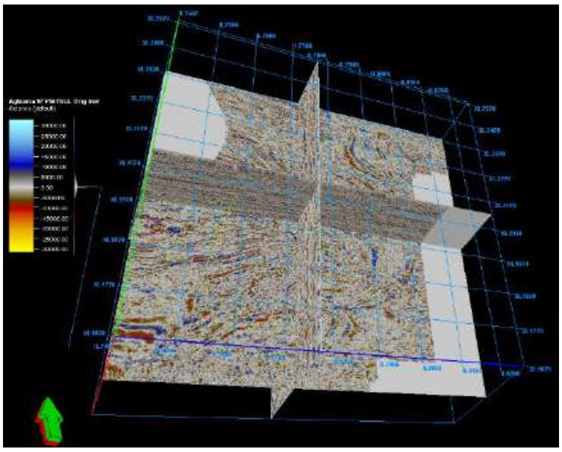

Figure 3: 3-D display of the seismic volume and the locations of the well data used in this study.

Methodology: The methods employed in this study took an integrated approach with iterative series of workflow between seismic and well data interpretation as presented in Figure 4.

Well-log Interpretation: The lithologic environment of the study area is a sand/shale sequence. Data used for the interpretation comprise gamma-ray logs with counts measured on the horizontal scale from 0 to 150 calibrated in standard American Petroleum Institute (API). A baseline of 65 API was chosen to discriminate between sands and shales. The sand/shale sequence makeschoosing a baseline value to discriminate between the two dominant lithologies easy. The gamma-ray facies cut-off applied in this study includes 0 – 65 API representing sandstone facies, 65 – 75 API representing siltstone facies and >75 API representing shale facies.

Table 1: The borehole data showing available log suites for the wells.

WELL ID	GR (API)	DT (us/ft)	LLD (ohm)	NPHI (v/v)	RHOB (G/cm^3)	Checkshot	Biostratigraphic Data
AM-1	Y	X	Y	X	X	X	Y
AM-2	Y	Y	Y	Y	Y	Y	Y
AM-3	Y	Y	Y	X	Y	Y	X
AM-4	Y	Y	Y	X	Y	X	X
AM-6	Y	X	Y	X	Y	Y	X
AM-7	Y	X	Y	X	X	X	X
AM-8	Y	X	Y	X	X	Y	X
AM-9	Y	X	Y	X	X	Y	X
AM-10	Y	X	Y	X	Y	x	X

Y = available, X = not available.(GR = Gamma Ray log, DT = Sonic log, LLD & LLS = Resistivity logs, NPHI = Neutron log, and RHOB = Density log).

The individual interpretations for each borehole were correlated across all the available boreholes to reveal the lateral and vertical variations of the lithologies, reservoirs and petrophysical properties.

Seismic-to-well tie: A synthetic seismogram is a modeled seismic trace derived from sonic and density logs. The synthetic seismogram allows well data recorded in units of depth to be compared to seismic data recorded in units of time. Synthetic Seismogram and seismic-to-well ties were generated for well AM-2 using sonic and density logs and time-depth relationship (TDR) from the checkshot data. Deterministic wavelet method was extracted from the seismic data and was used to convolve the reflection coefficients to generate the synthetics (Figure 5).

The seismic-to-well tie appears to be a very good tie. The top of the reservoirs correspond to a peak positive amplitude indicating high acoustic impedance sands.

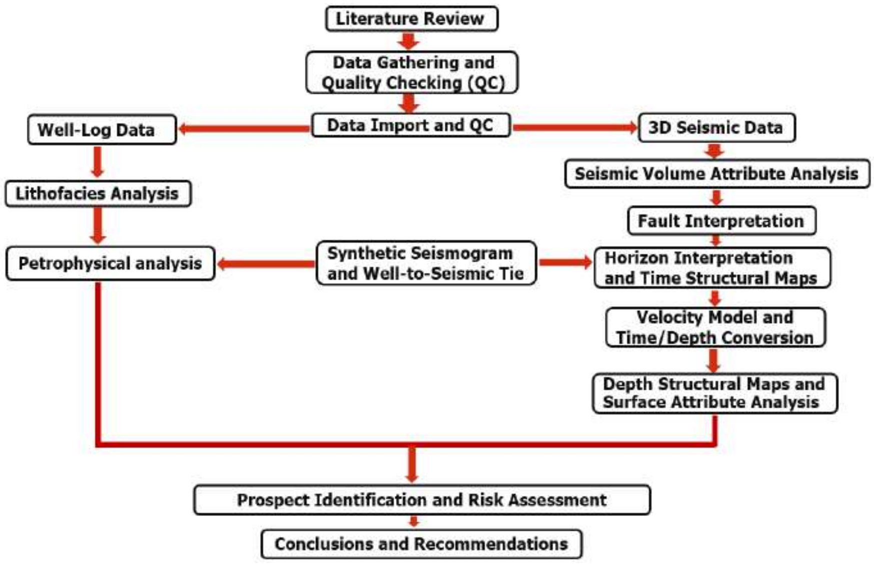

Figure 4: Workflow and methodology adopted for this study.

Seismic Interpretation: The structural and stratigraphic mapping was carried out using the 3-D seismic volume. Interpretation of the seismic data involves fault and horizon mapping across the seismic volume. Fault interpretation was carried out on every 5th inline. The variance (edge) volume attribute was used to validate the faults that were not visible on the original seismic data time slices. The visualization of these faults helped to interpret all the faults within the Agboma field. One horizon corresponding to the top of the AM-Prospect reservoir was mapped across the entire 3-D seismic volume. The identification and interpretation of the prospect are based on the interpretation of bright amplitudes which were further studied using RMS Amplitude and Sweetness attributes. The AM-Prospect horizon was mapped using manual tracking mode on the peak event at every 10th inline and crossline.

Time-depth conversion of time structural map of AM-Prospect was done by integrating TDR derived from checkshot data with the layer cake velocity model method (Eqn. 1).

$$V = V_0 + K*Z \text{.................. Eqn. 1 (Schlumberger, 2007a)}$$

Where V_0 = well TDR Surface, K = well TDR constant, Z = depth (ft).

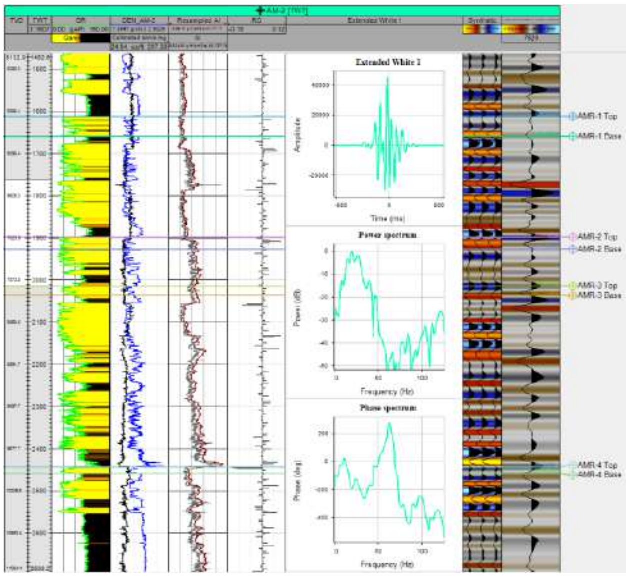

Figure 5: Synthetic seismogram generated using well AM-2 for the seismic-to-well tie.

Petrophysical Analysis: Petrophysical parameters were evaluated using Asquith's (2004) equations (Eqns. 2 – 10). The petrophysical parameters studied include:

a). volume of shale (Vsh), which was estimated from the gamma-ray log using Larionov's (1969) equation for Tertiary rocks (Eqns. 2- 3). The gamma-ray index was first calculated using equation 2.

$I_{GR} = \frac{GR_{log} - GR_{min}}{GR_{max} - GR_{min}}$ ……… (2)

$V_{sh} = 0.083\ (2^{(3.7 * IGR)} - 1)$ ………. (3): Larionov, 1969

Where: I_{GR} = Gamma-ray index, GR_{log} = Gamma ray log reading, GR_{min}= Minimum value of gamma-ray reading, GR_{max} = Maximum value of gamma-ray reading.

b). porosity is the ratio of voids to the total volume of rock and measures the fluid a rock will hold. It is quoted as a fraction or percentage. The effective porosity was evaluated from the bulk density log and fluid contents (Eqns. 4-5).

$\Phi_{den} = \frac{\rho_{ma} - \rho_b}{\rho_{ma} - \rho_f}$ ……… (4)

$\Phi_e = (1 - V_{sh}) * \Phi_{den}$.......... (5)

Where: Φ_{den} = Density porosity, ρ_{ma} = Matrix density (2.65 g/cm^3), ρ_b = Formation bulk density, ρ_f = fluid density (0.9 g/cm^3), V_{sh}= volume of shale.

c). Water and hydrocarbon saturations were estimated using the Archie (1942) model (Eqns. 6-7). Water saturation was evaluated from the true formation resistivity log (Rt) and the derived formation water resistivity (Rw).

$\mathbf{S_w} = \sqrt[n]{\frac{a \times R_w}{\Phi^m \times R_t}}$ …………(6): Archie, 1942

S_W = water saturation, n= saturation exponent taken as 2, a= empirical constant (1), R_W = resistivity of water formation, Φ = Porosity, m = Cementation exponent (2),R_t = true resistivity.

$S_h = (100 - S_w)$ % ……….. (7)

Where: S_W = Water saturation, S_h= hydrocarbon saturation

d). The permeability was estimated based on Timur's (1968) equation (Eqn. 8).

$K = (100 * \Phi_e^{2.25}) / S_{wirr}^2$ ……… (8): Timur, 1968

Where: S_{wirr}= Irreducible water saturation (0.15), Φ_e= Effective porosity, K = Permeability.

e). Reservoir net-to-gross determined from the gamma-ray log by estimating the ratio of the total thickness of sand facies to the gross thickness of the reservoir interval as presented in equation 9.

$NTG = T_n / T_g$………… (9)

Where: T_n = Net reservoir thickness, T_g= Gross reservoir thickness

The porosity, permeability, water saturation, hydrocarbon saturation, shale volume, and net-to-gross were computed to determine the reservoir quality of the sandstone intervals.

The original hydrocarbon-in-place (in barrels) was calculated using equation 10.

STOIIP = 7758 * A * H * ⍰ * Sh / Bo ……….. (10)

Where: STOIIP = stock tank oil in place (stb), A= area (acre), h = reservoir thickness (ft), ⍰ = rock porosity (%), Swc =connate water saturation (%), Boi = oil formation volume factor, rb/stb.

The Petrel software was used to carry out the detailed well-log interpretation, calculation of the petrophysical properties of the reservoirs, generation of the synthetic seismogram and seismic interpretation.

Results and Discussions

Well-log Interpretation

The potential reservoir sands decreased in thickness basin-ward from north to south as sands shaled out (yellow-coloured areas) while shales (potential source and seal) generally thinned out land-wards (black and light grey-coloured areas) (Figure 6). The shaly sequence basinward and the sandy sequence landward resulted from increasing marine activities basin-ward while fluvial activities dominate in the land-ward part of the study area. The reservoirs and seals are well distributed laterally across the study area. Hydrocarbon-bearing reservoirs identified are correlated across the available wells. They show good lateral continuity, with some reservoirs in the wells appearing wet, which may result from faults acting as barriers within the carrier beds (Figure 6).

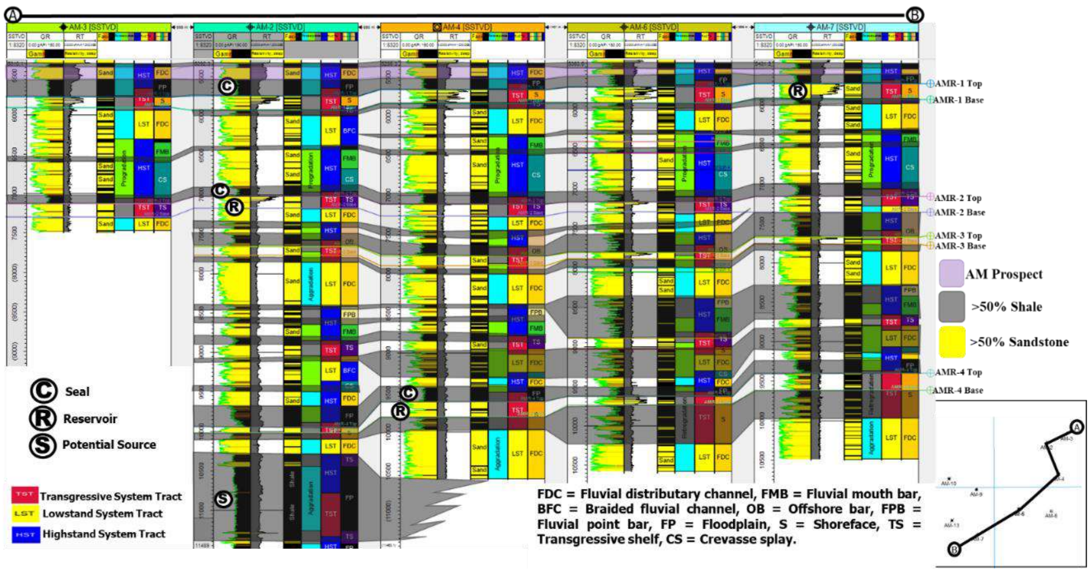

Figure 6: Lithofacies analysis showing the petroleum system elements distributions across the study area along depositional dip.

Four (4) hydrocarbon-bearing reservoirs named AMR-1, AMR-2, AMR-3 and AMR-4 and one prospect reservoir named AM-Prospect reservoir were identified and correlated across three wells (Figure 6). Stratigraphic correlations of delineated reservoirs were carried out to understand reservoirs' lateral and vertical continuity and terminations. The reservoirs are described and evaluated from the oldest (AMR-4) to the youngest (AMR-1) reservoir.

The Agboma Field stratigraphic intervals fall within the Paralic sequence of alternating sand and shale bodies of variable thicknesses. The entire sequence constitutes an overall prograding delta with periods of transgression. Log trends generally change from thicker, sandier, blocky and upward fining successions to thinner upward coarsening successions, suggesting a progression from channel deposits to dominantly offshore prograding lobes (Figure6). This succession reflects a progression from fluvial depositional settings to pro-delta and deltaic shorelines (Doust and Omatsola, 1990; Chima *et al*., 2017; Ogbe, 2020).

In order to integrate well data (measured in depth) and seismic data (in time) for accurate regional mapping of reservoir tops, a well-to-seismic tie was carried out. This was achieved using AM-2 well (see Figure 5), which has accurate checkshot data, and sonic and density logs required to generate a synthetic seismogram for well-to-seismic tie operation. Results of the seismic-to-well tie show that the top of the reservoirs corresponds to peak (positive amplitude) reflections which means that the AM Prospect reservoir's top is interpreted on a peak reflection.

Petrophysical Analysis and interpretation

Reservoir petrophysical parameters were calculated for all the reservoirs across three wells (AM-2, AM-4, and AM-6). The parameters calculated include reservoir thickness (gross and net), Volume of Shale (Vsh), Net-to-Gross (NTG), effective porosity (□), Water Saturation (Sw), permeability (K) and Hydrocarbon Saturation (Sh) (Figure 7). Tables 2 and 3 show the reservoir parameters calculated from the three wells for the four reservoirs and the AM-Prospect reservoir. Petrophysical calculations were carried out using equations 2 to 10, highlighted in the methodology section.

Reservoir AMR-1: is interpreted to be shaly with a good sand development throughout the reservoir region and a consistent lateral stratigraphy having an average gross thickness of 187.8 ft. The petrophysical evaluation reveals an average net reservoir thickness of 144.74 ft, and the average net-to-gross of the reservoir is 0.763 (76.3 %). The average porosity and permeability values of AMR-1 are 28.3 % and 1021.7 mD, respectively. The calculated porosity and permeability show that the reservoir is of good quality despite the average volume of shale of 23.7 %, as the reservoir consistently showed very high resistivity readings (Table 2 and Figure 7). The average hydrocarbon saturation of 74 % indicates that the reservoir holds a significant volume of hydrocarbon.The high shale content within the reservoir unit will likely provide permeability barriers limiting the fluid flow rate within the reservoir. Reservoir AMR-2 may have different flow units arising from the interbedding of the reservoir sandstones with the marine shale.

Reservoir AMR-2: this reservoir has a good sand development with intercalation of a shale unit that compartmentalised the reservoir, acting as a flow barrier (Figures 6 and 7). The reservoir is laterally consistent, with an average gross thickness of 141.98 ft. The petrophysical evaluation reveals an average net reservoir thickness of 128.68 ft with an average volume of shale of 10.3 %.The average net-to-gross of the reservoir is 89.7 %. The reservoir shows good quality with average porosity and permeability values of 27.7 % and 694.7 mD, respectively (Table 2). The average hydrocarbon saturation of 77.3 % indicates that the reservoir holds a significant volume of hydrocarbon in wells AM-2 and AM-6.The reservoir appears to be structurally controlled, with the middle well (AM-4) having a very low resistivity reading within the sand package (Figure 7).

Reservoir AMR-3: The reservoir constitutes very clean sands with an average gross and net thickness of 102 ft. Calculated average values of porosity, permeability, water saturation, hydrocarbon saturation, and net-to-gross are 25 %, 220 mD, 51.7 %, 49.3 %, and 100 % respectively (Table 2). The average hydrocarbon saturation of 49.3 % is an indication that the reservoir holds a small volume of hydrocarbon in AM-6 well while AM-2 and AM-4 wells are interpreted to be wet. In general, the reservoir shows good quality with average porosity and permeability values of 25 % and 220 mD respectively.

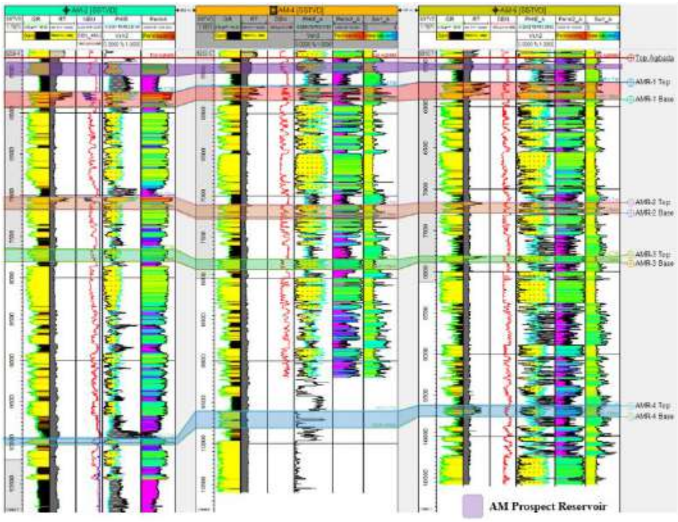

Figure 7: Petrophysical evaluation of the identified reservoirs correlated across AM-2, AM-4 and AM-6 wells.

The distribution of hydrocarbon in this reservoir is interpreted to be structurally controlled as two of the wells in up-dip section have very low resistivity values.

Reservoir AMR-4: the reservoir has an average gross thickness of 126.40 ft and an average net reservoir thickness of 110.38 ft. The average net-to-gross of the reservoir is 87.7 %. The average porosity and permeability values of AMR-4 are 19.5 % and 312 mD, respectively (Table 2).

Table 2: Summary of Petrophysical parameters calculated for reservoir AMR-1.

WELLS	Fluid Type	Tg (ft)	Tn (ft)	Vsh (%)	NTG (%)	ϕ (%)	K (mD)	Sw (%)	Sh (%)
Reservoir AMR-1									
AM-2	Oil	184.36	157.48	15	85	28	1517	26	74
AM-4	Oil	176.5	111.35	37	63	29	631	28	72
AM-6	Oil	202.46	165.39	19	81	28	917	24	76
Average		187.8	144.74	23.7	76.3	28.3	1021.7	26	74
Reservoir AMR-2									
AM-2	Oil	151.01	151.01	0	100	28	1681	16	84
AM-4	Oil	152.12	141.53	7	93	30	46	25	75
AM-6	Oil	122.82	93.5	24	76	25	357	27	73
Average		141.98	128.68	10.3	89.7	27.7	694.7	22.7	77.3

Reservoir AMR-3									
AM-2	Oil	107.62	107.62	0	100	13	65	100	0
AM-4	Oil	122.24	122.24	0	100	30	54	26	74
AM-6	Oil	76.13	76.13	0	100	31	541	29	74
Average		102	102	0	100	25	220	51.7	49.3
Reservoir AMR-4									
AM-2	Oil	73.35	73.35	0	100	12	35	100	0
AM-4	Oil	192.54	177.06	8	92	NA	NA	100	0
AM-6	Oil	113.3	80.73	29	71	27	589	29	71
Average		126.40	110.38	18.5	87.7	19.5	312	76.3	23.7

(Tg = gross thickness, Tn = net thickness, Vsh = volume of shale, NTG = net-to-gross, ⍰ = porosity, K = permeability, Sw = water saturation and Sh = hydrocarbon saturation).

The estimated porosity and permeability show that the reservoir is of good quality, with an average volume of shale of 18.5 %. The reservoir consistently showed low resistivity readings in AM-2 and AM-4 (Figure 7). In AM-6 well, the reservoir appears shaly, which affected the volume of fluid content. The average hydrocarbon saturation of 23.7 % indicates that the reservoir does not hold a significant volume of hydrocarbon.

Seismic attribute analysis and structural Interpretation

Analysis of the structural framework of the Agboma Field includes evaluation of the faulting system and how they have affected the stratigraphic packages within the field. To accurately interpret the structural framework, we first carried out a Variance (edge) volume attribute analysis to better reveal the faults within the interval of interest. The Variance (edge) attribute was selected due to its relatively high accuracy in revealing faults and fractures, including those that are below seismic resolution known as sub-seismic faults. Variance (edge) attribute time slices were generated at various times and used as a guide to interpreting the faults throughout the entire seismic volume along seismic inline which clearly shows zones of stratigraphic discontinuities (Figure 8). Variance (edge) values of 0.50 to 1 indicate stratigraphic discontinuities and the presence of faults.

RMS and Sweetness volume attributes were extracted from the original seismic volume and time slices were generated from the attribute volumes at different seismic depths to detect the presence of hydrocarbon accumulations (Figures 9 and 10). The amplitude anomalies were identified based on their response to the seismic attributes which are indicative of the presence of hydrocarbon accumulation. Figure 9a show the original seismic data with localized high and low amplitude variations. The amplitude variations did not represent the true geometry of the reservoir (Figure 9b). The RMS amplitude is displayed in Figure 9c-e. High values of the RMS amplitude are related to porous sands which are high quality hydrocarbon reservoirs (Chopra and Marfurt, 2007; Azevedo, 2009; Nwaezeapu et al., 2017). The localized higher amplitude zones suggest the presence of hydrocarbon charged reservoir. Amplitude variations within the amplitude maps suggest variability in the lithology. The sweetness attribute which combines amplitude and frequency of the seismic data shows sweet spot zones that correspond to the localized higher amplitudes observed in the RMS amplitude map (Figure 10).

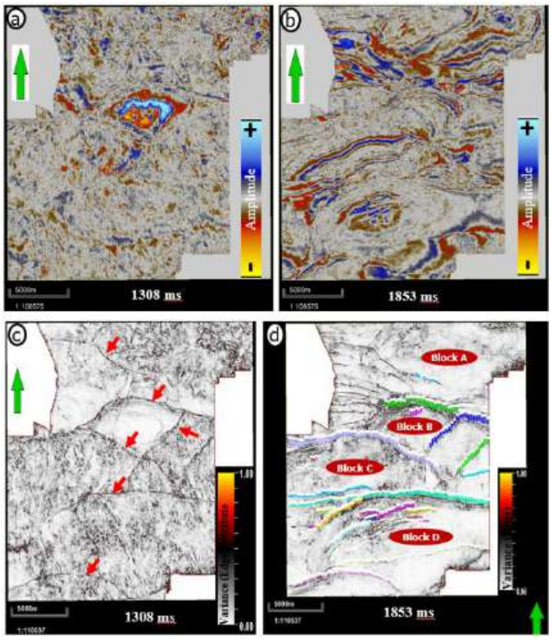

Figure 8: Structural interpretation using volume attribute analysis. (a) and (b). Original seismic time slices at 1308 ms and 1853 ms respectively show a lack of faults. (c). Variance (edge) attribute time slice at 1308 ms showing the structural architecture of the field. The red arrows point to faults. (d). Variance (edge) attribute slice at 1853 ms showing interpreted faults and the subdivision of the field into four distinct blocks separated by the major faults in the field.

The results show very strong localized high RMS amplitudes and sweetness values confined within faults in fault block B and C which suggest the presence of hydrocarbon confined within structural closures (Figure 9 and 10). The interpretation of accumulation was further strengthened by the presence of direct hydrocarbon indicators such as dim spots, flat spot and localized bright amplitudes corresponding to sand deposits.

Altogether, total of twenty-five (25) faults were identified and mapped in the study area out of which seventeen were observed to cut through the AM-Prospect reservoir. The faults are grouped into major and minor faults with the major faults compartmentalizing the field into four fault blocks labelled block A, block B, block C and block D. The major faults extended up to 3250 ms after which they sole out (Figure 11). The faults trend in the east-west direction and downthrown southwards. The minor faults are interpreted as synthethic (basin-ward direction of the fault plane) normal faults and antithetic (land-ward direction of the fault plane) normal faults.

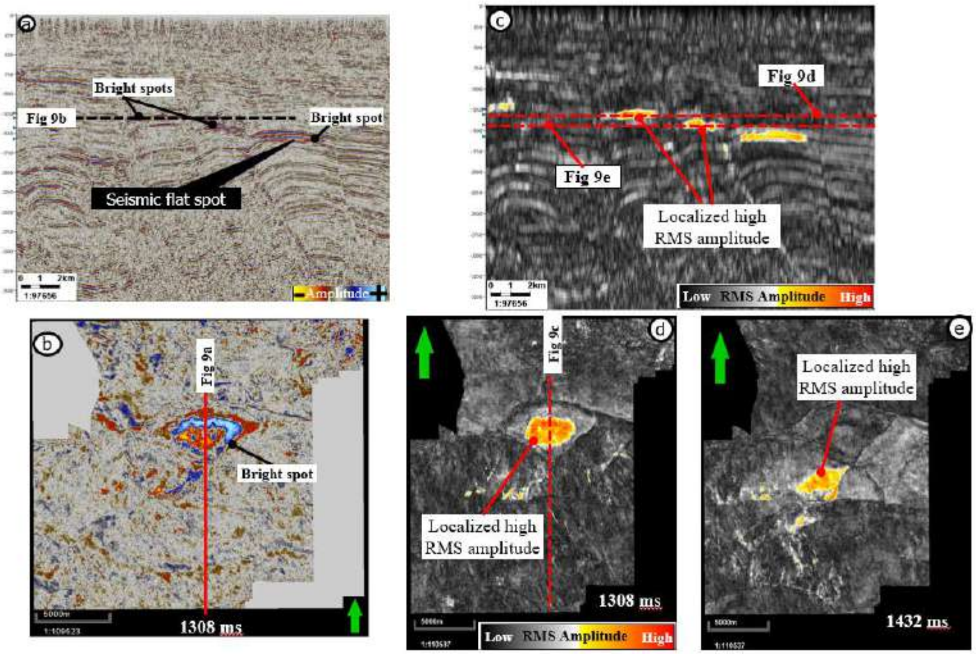

Figure 9: Prospecting for new exploration targets. (a) Original seismic showing flat spot and bright spots which are direct hydrocarbon indicators (DHIs). (b) Shows the time slice at 1308 ms showing the distribution of the bright spot in plane-view. (c) RMS amplitude attribute showing anomalously high amplitudes corresponding to zones with bright spots. (d) and (e) shows the distribution of RMS amplitude in plane-view as it relates to fluid saturation extent at time slices 1308 ms and 1432 ms respectively.

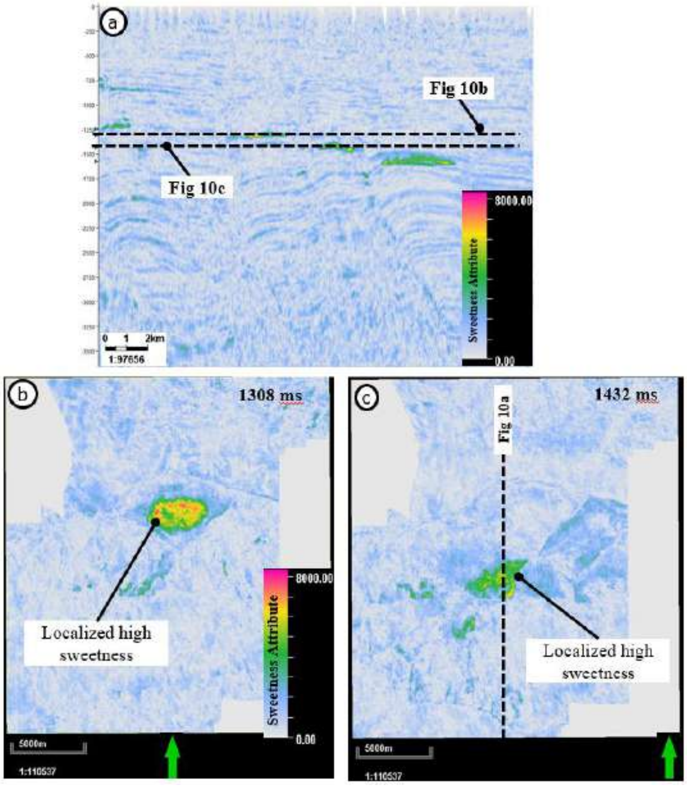

Figure 10: Prospecting for new exploration targets. (a) Sweetness attribute showing porous sandstone units corresponding to zones with bright spots. (b) and (c) shows the distribution of sweetness attribute in plane-view as it relates to reservoir extent at time slices 1308 ms and 1432 ms respectively.

One key horizon named AM-Prospect reservoir was mapped across the entire seismic volume to generate the time surface map of the reservoir (Figures 11b and 12a). The time surface map was depth converted to get the drillers depth since drilling takes place in the depth domain and is shown in Figure 11b. The depth map of AM-Prospect reservoir shows structural closures which are mainly four-way anticlinal dip structural closure (AM-Prospect 1a) and two-way fault dependent structural closure (AM-Prospect 1b) (Figure 12b). These structural closures are potential sites for hydrocarbon accumulation especially where the faults are sealing.

The trapping styles identified in this study for the AM-Prospect include simple rollover anticlinal trap and regional foot wall structure trap. Hydrocarbon migration are inferred to be through the faults and within the carrier beds (Figure 13). The petrophysical reservoir evaluation has analysed and quantified the reservoir properties of the identified reservoirs and prospect. Using the depth structural map, it is now possible to assess the production potential in the two target structures labelled AM Prospect 1a and 1b and the calculation of STOIIP (eqn. 10) is utilized to assess how much oil is thought to be in place.

Structural Framework and Hydrocarbon Prospectivity
The study area which is situated in the western Coastal Swamp Depobelt of the Niger Delta Basin is bounded by three major down-to-basin normal faults. Structural interpretation across the field revealed the presence of down-to-basin normal faults with associated rollover anticlines, synthetic and antithetic normal faults. The major down-to-basin faults subdivided the field into four fault blocks and acts as the primary hydrocarbon migration route in the field (Figures 13). The key implication of the structural framework is that faults created bulk of the accommodation space for sediment deposition as sediments were observed to thicken across the major faults with significant throws.
The key significant aspect of this study is the identification and assessment of new hydrocarbon prospects within the undrilled fault blocks B and C labelled AM-Prospect 1a and 1b based on structural closures identified on the depth structure map the AM-Prospect reservoir (Figure 12b). RMS amplitude surface attribute extraction confirms the existence of hydrocarbon accumulations within the structural closures identified as four-way anticlinal trap and two-way fault dependent trap. The conformity of bright amplitudes within the trapping structures supports the interpretation of hydrocarbon accumulation in fault blocks B and C (Figure 14).

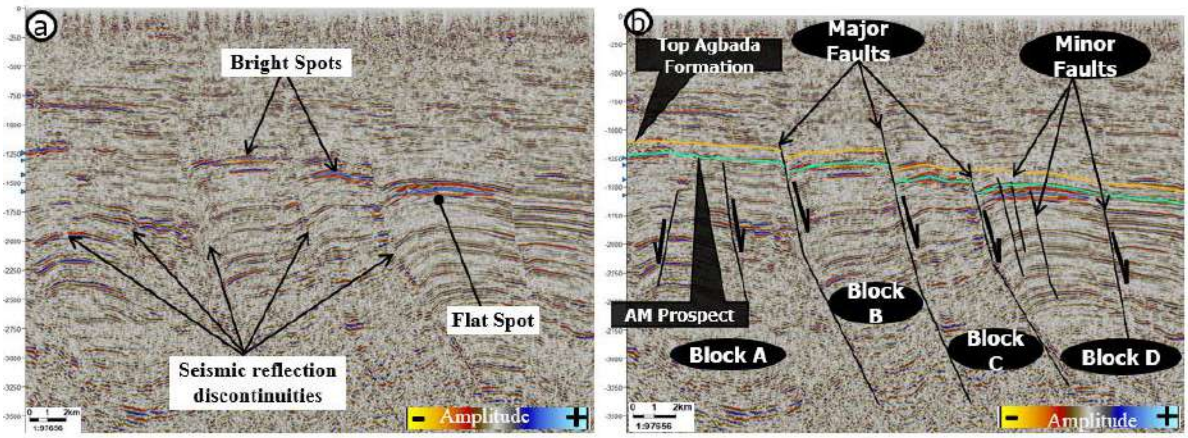

Figure 11: (a) Uninterpreted seismic section at inline 7900 showing seismic reflection discontinuities and direct hydrocarbon indicators in the study area. (b) Interpreted seismic section showing the mapped faults and horizons.

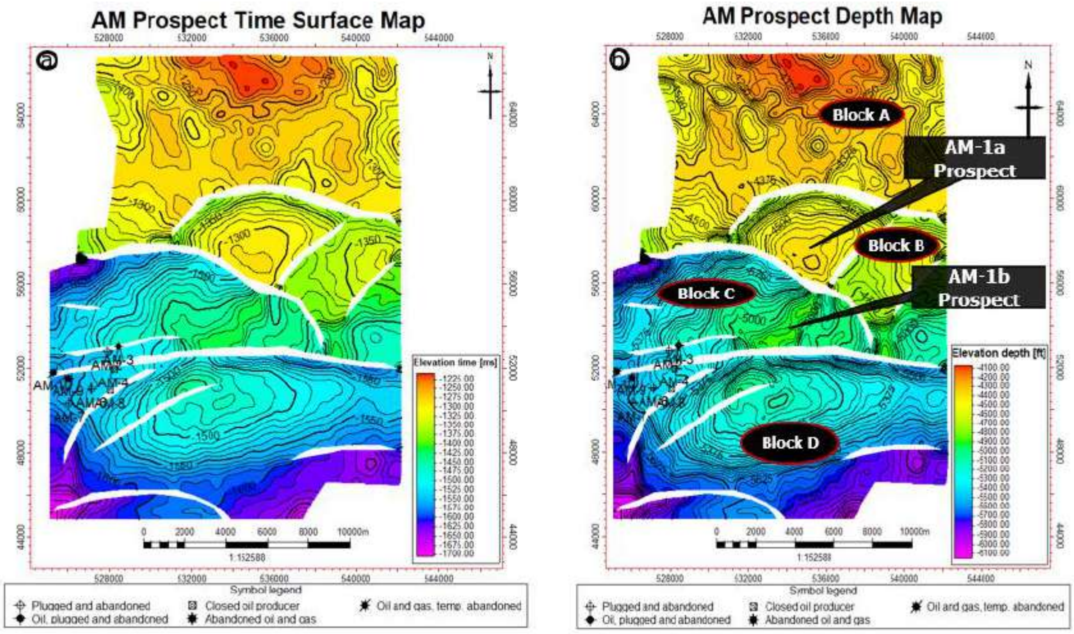

Figure 12: (a) Time structural map of AM Prospect reservoir top. Contour interval is 25 ms. (b) Depth structural map of AM Prospect reservoir top converted using layer cake velocity model. Contour interval is 100 ft.

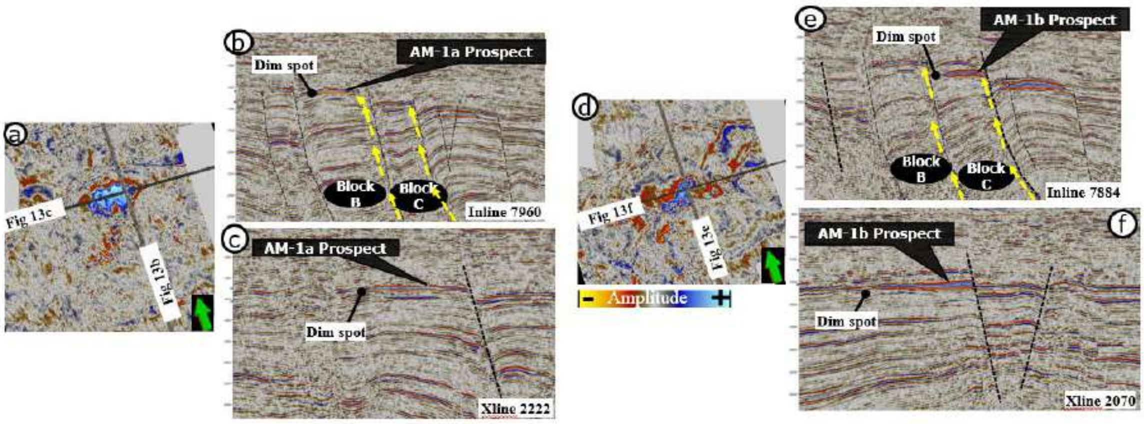

Figure 13: (a) time slice 1300 ms showing localised high amplitudes. (b) and (c) shows the structural control for AM Prospect 1a at inline 7960 and crossline 2222 respectively. (d) Time slice 1424 ms showing localized high amplitudes for AM Prospect 1b. (e) and (f) shows the structural control for AM Prospect 1b at inline 7884 and crossline 2070 respectively. Yellow arrows inferred fluid migration pathway through the faults.

AM Prospect Reservoir Petrophysical Evaluation: The petrophysical evaluation reveals an average gross and net reservoir thickness of 118 ft., and an average net-to-gross of 100 % (Table 3) The average hydrocarbon saturation of 74 % is an indication that the reservoir prospect holds a significant volume of hydrocarbon. In general, the reservoir shows good quality with average porosity and permeability values of 26 % and 715 mD respectively (Table 3).

Table 3: Summary of Petrophysical parameters calculated for reservoir AM-Prospect reservoir.

WELLS	Fluid Type	Tg (ft)	Tn (ft)	Vsh (%)	NTG (%)	ϕ (%)	K (mD)	Sw (%)	Sh (%)	Bo (rb/stb)	Area (acre)	STOIIP (MMSTB)
AM-Prospect 1a	Oil	118	118	0	100	26	715	26	74	1.29	2380.8	325.1
AM-Prospect 1a	Oil	118	118	0	100	26	715	26	74	1.29	2692	367.6

(Tg = gross thickness, Tn = net thickness, Vsh = volume of shale, NTG = net-to-gross, ⍰ = porosity, K = permeability, Sw = water saturation and Sh = hydrocarbon saturation, Bo = oil formation volume factor, STOIIP = stock tank oil in place).

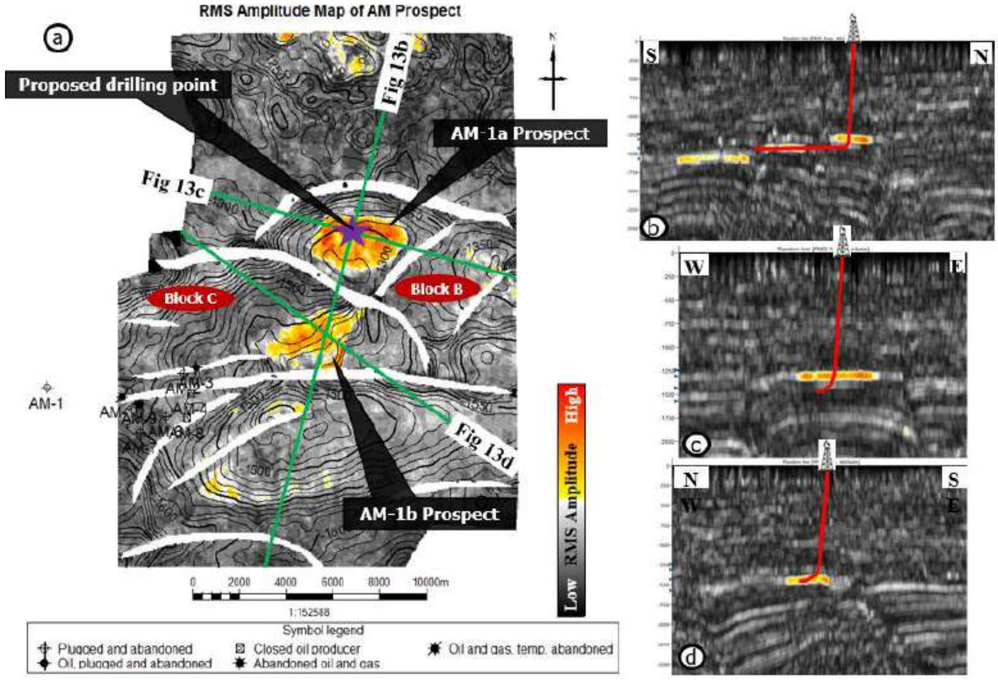

Figure 14: (a) RMS Amplitude map of AM Prospect showing localised high amplitudes indicative of hydrocarbon accumulations within fault blocks B and C. (b), (c) and (d) shows the seismic transects across the two targetsand the trajectory of the proposed well.

Conclusions

To revitalize and optimize production, and contain the hydrocarbon production decline in Agboma Field, integration of lithofacies, petrophysical, seismic attribute and structural analysis have been successfully employed in this study. The deliverables this study achieved are summarized as follows:

1). The correlation of the identified reservoirs across available wells along depositional dip shows that the reservoirs are laterally continuous with varying thicknesses at borehole points. Petrophysical analysis shows that the reservoirs are generally characterised by a high net-to-gross ratio. AMR-1, AMR-2, and AM-Prospect reservoirs have excellent reservoir properties with average hydrocarbon saturation of 74%, 77.3% and 74%; average porosity of 28.3%, 27.7%, and 26%; and permeability of 1021.7 mD, 694.7 mD, and 715 mD respectively. The volumetrics indicate that the AM-Prospect reservoir is prolific and commercially viable for the marginal oil field operation with STOIIP of 325.1 MMSTB and 367.6 MMSTB for AM Prospect 1a and 1b respectively.2). The structural framework of Agboma field is controlled by extensional tectonics. Three major faults and twenty-two minor faults were interpreted to offset the stratigraphic packages within the field at different seismic depths. The faults created structures that are favourable for hydrocarbon migration and accumulation. Attribute analysis and interpreted surface maps document structural closures that indicate the existence of hydrocarbon prospects within the field.

3. Surface attribute analysis of the prospects are essentially characterized by fault-dependent closures and the RMS Amplitude attribute show that the engagement of the closures are not strongly dependent on the sealing capacities of the bounding faults. The closures appear to be rollover-anticlinal at the crest.

Acknowledgement
We want to thank Shell Petroleum Development Company (SPDC) PortHarcourt for providing the dataset used in this study and Schlumberger for using the Petrel Software donated to the Department of Geological Sciences, Nnamdi Azikiwe University, Awka.

References

Ahaneku, C. V., Okoro, A. U., Odoh, B. I., Anomneze, D. O., Chima, K. I., Ejeke, C. F., and Okoli, I. N., (2016). Sequence Stratigraphy, Structural framework and hydrocarbon migration of Ariki field, Nigeria. Petroleum Exploration and Development, 43(1), 82-88.

Ajakaiye, D. E. and A. W. Bally, (2002a). Course Manual and Atlas of structural styles on reflection profiles from the Niger Delta: American Association of Petroleum Geologists Continuing Education course note series 41, 107.

Amigun, J. O., Olisa, B. and Fadeyi, O. O. (2012). Petrophysical analysis of well logs for reservoir evaluation: a case study of Laja Oil Field, Niger Delta. J. Pet. & Gas Explor. Res. 2(10), 181 -187.

Aniefiok, E. I., Udo, J. I., Margaret, U. I., and Sunday W. P., (2013). Petroleum Exploration: Past and Present Environmental issues in the Nigeria Niger Delta. American Journal of Environment Protection, 1 (4), 78-90.

Archie, G. E., (1942). The electrical resistivity log as an aid in determining some reservoir characteristics. J. Petroleum Technol., 5: 54-62

Asquith G, Krygowski D (2004): Basic Well Log Analysis: AAPG Methods in Exploration Series. 16p.

Azevedo, L., (2009). Seismic attributes in hydrocarbon reservoirs characterization. Universidade de Aveiro, Department de Geociencias. Unpublished Masters thesis.

Chima, K. I., Ozumba, B. M., Adejinmi, K. T., Hoggmascall, N. M., Orajaka, I. P., Okoro, A. U., and Ahaneku, C. V., (2017). Sequence Stratigraphy and Structure of the Southern Coastal Swamp of the Niger Delta, Nigeria: A new insight into the hydrocarbon systems and prospectivity at deeper stratigraphic interval. Journal of Applied Geology and Geophysics. 5(6), 32 - 47

Doust, H. and Omatsola,E. (1990). Niger Delta. In; J.D. Edwards and Santogrossi. (Eds.), Divergent/Passive Margins basin. American Association of Petroleum Geologist Memoir 48, 201-238.

Evamy, B.D., Haremboure,J., Kammerling,R., Knaap, W.A., Molloy,F.A., and Rowlands, P.H., (1978). Hydrocarbon habitat Tertiary Niger Delta, American Association of Petroleum Geologists, Bulletin, 73, 143-154.

Kulke, H., (1995). Nigeria, In; Kulke, H., (ed); Regional Petroleum Geology of the World. Part 11: African, American, Australian, and Antarctica: Berlin, GebruderBorntrager, 143-172.

Larionov V. V., (1969). Borehole Radiometry: Moscow, USSR, Nedra. Morris RL, Biggs WP (1967) "Using log-derived values of water saturation and porosity". Trans. SPWLA Ann. Logging Symp. Paper, 10: 26.

Mode, A.W., Anyiam, A.W. and Omuije, J.O. (2015). Analysis of Sedimentary facies and Paleodepositional Environments of the Dc70X reservoir in Mbakan field, Central Swamp, Niger Delta, Arabian Journal of Geoscience, 8(9), 7435 – 7443.

Nwaezeapu, C.V., Okoro, A.U., Unuevho, I.C., Chukwusa, U., Odika, F.N., Ahaneku, V.C., and Okoye, C.C., (2017). Seismic volume attribute analysis for structural and leads identification: a case study of Chiadu Field, onshore Niger Delta Basin, Nigeria. International Journal of Science and Technology. 6(9), 904 – 912.

Nwozor, K. R., Omudu M. I., Ozumba B. M., Egbuachor, C. J., Onwuemesi, A. G., and Anike O. L., (2013). Quantitative evidence of secondary mechanisms of overpressure generation: Insights from parts of Onshore Niger Delta, Nigeria, Journal of Petroleum Technology Development, 3 (1), 64-83.

Obiadi, I. I., Okoye, F. C., Obiadi, C. M., Irumhe, P. E., and Omeokachie, A. I., (2019). 3-D structural and seismic attribute analysis for field reservoir development and prospect identification in Fabianski Field, onshore Niger Delta, Nigeria. Journal of African Earth Sciences, 158, 103562.

Ogbe, O.B. (2020). Sequence stratigraphic controls on reservoir characterisation and architectural analysis: A case study of Tovo field, coastal swamp depobelt, Niger Delta Basin, Nigeria, Marine and Petroleum Geology. doi: https://doi.org/10.1016/j.marpetgeo.2020.104579.

Omatsola, E., (2013). The Niger Delta is not a mature Basin. Africa oil and gas report. June 28, 2013.

Reijers, T.J., Petters, S.W. and Nwajide, C.S. (1997). The Niger Delta. In R. E. Selley, African Basins-Sedimentary Basin of the World 3. Amsterdam: Elsevier Science, 151-172.

Short, K. C., and Stauble, A. J., (1967). Outline of Geology of Niger Delta. American Association of Petroleum Geologist Bulletin, 51, 761-779.

Timur A (1968). An investigation of permeability, porosity, and residual water saturation relationships for sandstone reservoirs. Log Analyst, 9: 8 – 17

Xiao, H., and J. Suppe, (1992). Origin of rollover: American Association of Petroleum Geologists Bulletin, 76, 509-229.